

Atomic-resolution structure of the cellulose synthase regulator cyclic diguanylic acid

(RNA/x-ray crystallography/G-G base pairs/hydrogen bonding)

MARTIN EGLI*, REINHARD V. GESSNER*, LOREN DEAN WILLIAMS*, GARY J. QUIGLEY†, GIJS A. VAN DER MAREL‡, JACQUES H. VAN BOOM‡, ALEXANDER RICH*, AND CHRISTINE A. FREDERICK*

*Department of Biology, Massachusetts Institute of Technology, Cambridge, MA 02139; †Department of Chemistry, Hunter College, New York, NY 10021; and ‡Gorlaeus Laboratories, Leiden State University, 2300RA Leiden, The Netherlands

Contributed by Alexander Rich, February 21, 1990

ABSTRACT Cyclic diguanylic acid acts as a regulator for cellulose synthase activity in the bacterium *Acetobacter xylinum*. We report the x-ray crystal structure of the regulator at atomic resolution. The structure contains two independent molecules that adopt almost identical conformations. The two molecules form self-intercalated units that are stacked on each other. Two different G-G base-pairing modes occur between the stacks. The more stable one has two or possibly three hydrogen bonds between two guanines and is related to the type of hydrogen bonding that is believed to exist between G-rich strands at the ends of chromosomes.

Low molecular weight nucleic acids regulate a diverse array of biological processes. GTP and cyclic (3',5') AMP help transmit information from cell surface receptors to nuclear DNA. ATP is required for energy exchange in nearly all biological systems and ppGpp and pppGpp are important in signaling a response to cellular stress. Cyclic diguanylic acid (c-di-GMP, Fig. 1), whose x-ray crystal structure is reported here, activates biosynthesis of cellulose in the Gram-negative bacterium *Acetobacter xylinum* (1). The c-di-GMP is formed by diguanylate cyclase in a two-step reaction: two molecules of GTP are first converted to the 5'-triphosphate dimer pppGpG, which is then condensed intramolecularly to c-di-GMP. The formation of c-di-GMP is strongly dependent on the cellular Ca^{2+} concentration. Association of c-di-GMP with the cellulose synthase then activates the enzyme.

Smaller nucleic acid molecules have been an important source of high-resolution structure information that contributes to the understanding of larger nucleic acids. The hydrogen bonds between guanines in the c-di-GMP crystal may help us understand a variety of nucleic acid complexes, including triple-strands and telomeres. Triple-stranded regions of DNA (2, 3) may play a role in the regulation of transcription and replication. Telomere DNA, which mediates association of chromosomes during mitosis and meiosis (4), may form inter- and intrastrand complexes from single-stranded G-rich repeats (5, 6).

EXPERIMENTAL PROCEDURES

Crystallization and Data Collection. c-di-GMP was prepared as described (1). Crystals were grown at room temperature from a solution containing 3.3 mM c-di-GMP, 50 mM sodium cacodylate (pH 6.5), 63 mM $MgCl_2$, and 3% 2-methyl-2,4-pentanediol, equilibrated against 40% 2-methyl-2,4-pentanediol by the sitting-drop vapor diffusion technique. Square-bipyramidal crystals began to appear after 3 months. Their space group was tetragonal $I4_1$ with unit cell dimensions $a = b = 20.061 \pm 0.003$ Å and $c = 39.402 \pm 0.006$ Å. On the

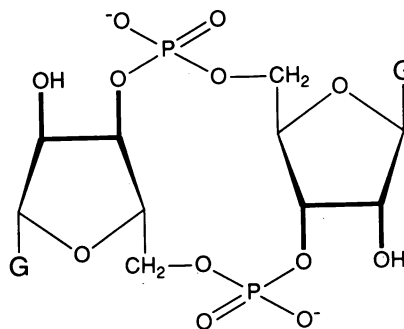


FIG. 1. c-di-GMP.

basis of the unit cell volume of $15,856 \pm 4$ Å³, two independent molecules per asymmetric unit were assumed. A crystal with approximate dimensions $0.2 \times 0.2 \times 0.4$ mm was sealed in a 0.2-mm glass capillary with a droplet of mother liquor and data were collected at $-10^\circ C$ on a rotating-anode four-circle diffractometer (Rigaku AFC5R) with graphite-monochromatized Cu $K\alpha$ radiation by the ω scan method. A total of 5145 unique reflections to better than 0.9-Å resolution ($2\theta = 120^\circ$) were collected, of which 3192 were observed above the $6\sigma(F_{obs})$ level (300 between 1.0- and 0.9-Å resolution). The maximum decay during the measurement was $<2\%$. Lorentz and polarization corrections were applied and an empirical absorption correction was used (7).

Structure Solution and Refinement. The structure was solved with the direct methods program SHELXS-86 (8), using an extended number of phase-generation cycles. Fourier maps revealed one complete molecule and both guanines as well as parts of the ring system of a second molecule. The missing atoms were generated by superimposing the complete molecule on the fragments of the second one. Initially, the structure was refined with the Hendrickson-Konnert least-squares refinement procedure (9) as modified for nucleic acids (G.J.Q., unpublished work). The constraints were gradually released and higher-resolution data were included as more and more water molecules were located in sum ($2F_{obs} - F_{calc}$) and difference ($F_{obs} - F_{calc}$) Fourier maps, displayed on an Evans & Sutherland PS390 graphics terminal with the program FRODO (10). The structure was then refined without constraints by block-matrix least-squares refinement with programs SHELX76-400 (11) and BIGSHELX-76 (12), which are updated versions of SHELX-76 (13). All RNA atoms, the magnesium ions, and the water molecules coordinated to them were refined anisotropically, whereas the isotropic displacement parameters of the additional waters were kept at a value of 0.25. The positions of the hydrogen atoms of the RNA dimers with the exception of the hydroxyl hydrogens were calculated and their isotropic displacement parameters

The publication costs of this article were defrayed in part by page charge payment. This article must therefore be hereby marked "advertisement" in accordance with 18 U.S.C. §1734 solely to indicate this fact.

Abbreviation: c-di-GMP, cyclic diguanylic acid.

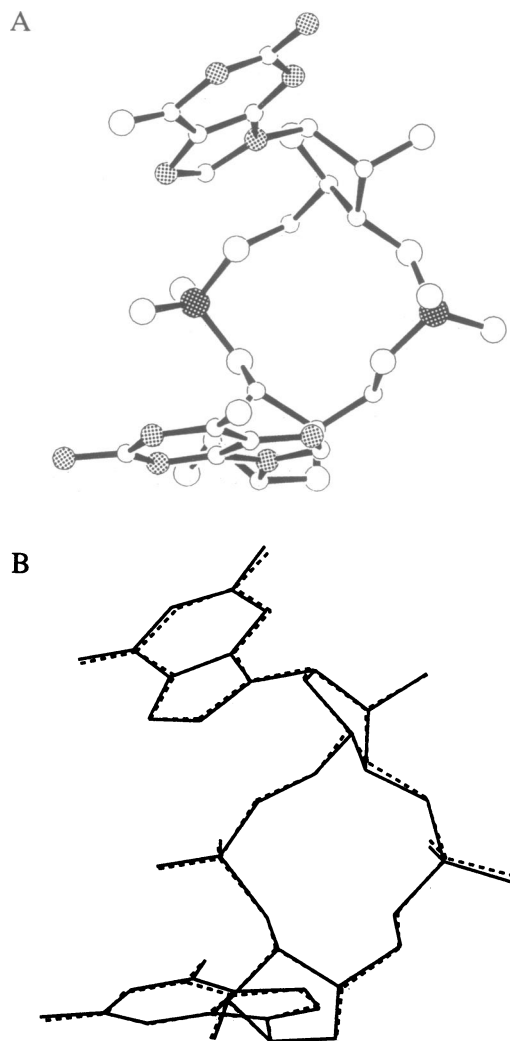


FIG. 2. (A) An ORTEP (14) drawing of molecule 1 of c-di-GMP. Nitrogens are stippled black-on-white; phosphorus atoms are stippled white-on-black. (B) Superposition of the two independent molecules of c-di-GMP. Molecule 1 is drawn with solid lines.

were fixed. C—H and N—H bond distances were 1.08 Å and 1.01 Å, respectively. Hydrogens for the water oxygens were not included. The final asymmetric unit contained 121 heavy atoms including two partially hydrated magnesium ions and 27 water molecules. The final weighted *R* factor [$1/\sigma^2(F_{\text{obs}})$ weights] was 9.4%, including 3877 reflections with $F_{\text{obs}} \geq 2\sigma(F_{\text{obs}})$ at full resolution. The coordinates will be deposited in the Cambridge Structural Database (Cambridge Crystallographic Centre, Cambridge, U.K.).

RESULTS

The c-di-GMP molecule contains two phosphodiester linkages. The first, like the phosphodiester backbone within

Table 1. Backbone torsion angles for c-di-GMP

Base*	Angle, degrees					
	α	β	γ	δ	ϵ	ζ
1	72.4	-167.2	51.9	90.9	-159.3	63.8
2	72.6	-167.1	49.8	91.0	-159.5	66.7
3	68.1	-169.1	59.9	78.1	-157.2	74.5
4	69.6	-167.5	52.4	87.7	-161.0	68.8

The standard angular notations are as follows: O3'—P ^{α} O5'—P C5'—C4'—C3'—O3'—P.

*Residues 1 and 2 form molecule 1, and residues 3 and 4 form molecule 2.

DNA and RNA, links O3' of one residue to P of the next residue, while the second links O3' of that residue back to P of the first residue, resulting in a symmetric cyclic phosphodiester backbone, forming a 12-membered ring. The conformation of one of the two crystallographically independent c-di-GMP molecules is shown in Fig. 2A. The values for the individual torsion angles of both molecules are listed in Table 1. The torsion-angle pairs α/ζ are gauche(+)/gauche(+) for both residues, as previously predicted for a nucleic acid chain that folds back on itself (15). The absence of deviations from standard backbone torsion angles in the 12-membered rings suggests that the rings close easily, with minimal torsional stress. A nearly perfect twofold symmetry is maintained by the backbone atoms, indicating that the conformations of the two residues in each ring are very similar.

The two crystallographically independent molecules have very similar conformations as illustrated by their least-squares superposition (Fig. 2B). All the riboses adopt a 2'-exo/3'-endo conformation, as expected for RNA. The individual sugar torsions are listed in Table 2. The intramolecular twofold symmetry is broken by the glycosyl torsion angle. The guanines are in two different orientations relative to the backbone ring. Thus, the bases are not parallel but are skewed at an angle of 25°. Both guanines of c-di-GMP are in the anti conformation, although the values of the glycosyl torsion angles χ vary by about 30°.

The two c-di-GMP molecules form an intercalated unit stabilized by stacks of four guanine bases such that the imidazole ring of one guanine is positioned over the pyrimidine ring of the next. The intercalated molecules are related by a noncrystallographic twofold axis through the magnesium ion as seen in Fig. 3A. Each outer guanine of the four-member stack is nearly coplanar with the adjacent base in the stack. However, the two central bases are not coplanar but are partially unstacked with a dihedral angle of 29°. The roll of the planes of the guanine bases opens a cleft in the center of the complex (Fig. 3C). The central bases of the stack appear as a "V" with the apex (directed at the viewer, Fig. 3B) composed of two N7 atoms. A Mg²⁺ ion is coordinated to these two N7 atoms. The Mg—N7 distances are 2.26 and 2.29 Å and the distance between the nitrogen atoms is 2.93 Å. The wedge shape of the two central bases resulting from the Mg²⁺ coordination induces a bend in the stacking of the intercalated unit. This bending in combination with the lattice

Table 2. Sugar torsion angles* (ν), pseudorotation phase angle (*P*), and glycosyl torsion angle† (χ) for c-di-GMP

Base	Angle, degree(s)						χ
	ν_0	ν_1	ν_2	ν_3	ν_4	<i>P</i>	
1	3.9	-28.2	41.3	-39.8	24.2	14	-151.9
2	15.5	-34.7	40.5	-34.8	11.4	-2	178.6
3	4.8	-26.0	32.7	-32.6	15.6	10	-157.3
4	11.5	-30.8	36.2	-31.7	12.7	1	178.5

*The standard angular notations are as follows: O4'—C1' ^{ν_0} —C2' ^{ν_1} —C3' ^{ν_2} —C4' ^{ν_3} —O4'.

†For purines, the glycosyl torsion angle is defined as angle O4'—C1'—N9—C4.

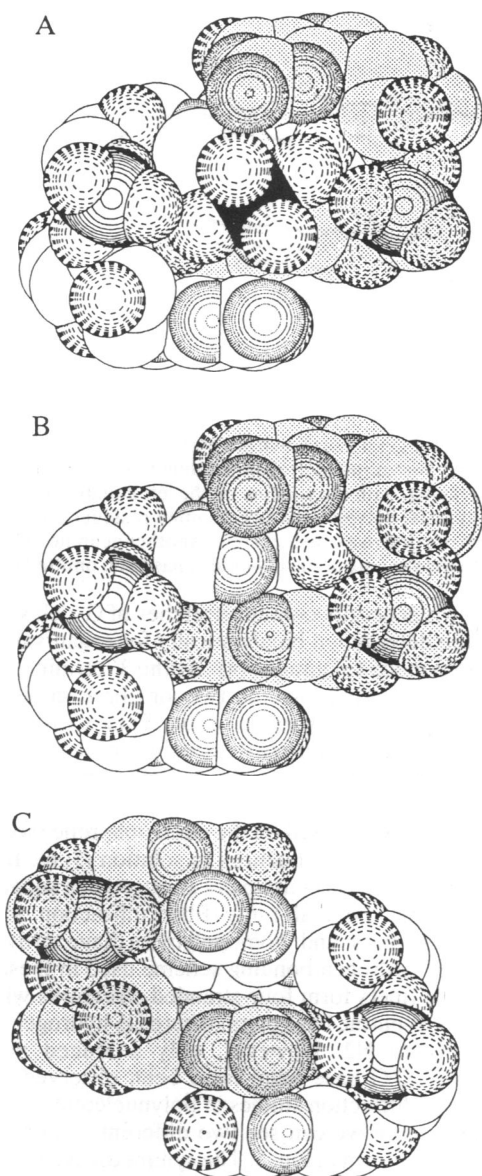


FIG. 3. Space-filling representations of the two self-stacked *c*-di-GMP molecules, with one molecule shaded. (A) Including the hydrated Mg^{2+} . (B) Same view as A with the hydrated Mg^{2+} omitted. (C) Rotated 180° about the vertical axis relative to A. Oxygen atoms are highlighted with dashes, nitrogen atoms with dots, and phosphorus atoms with solid lines; the Mg^{2+} is black.

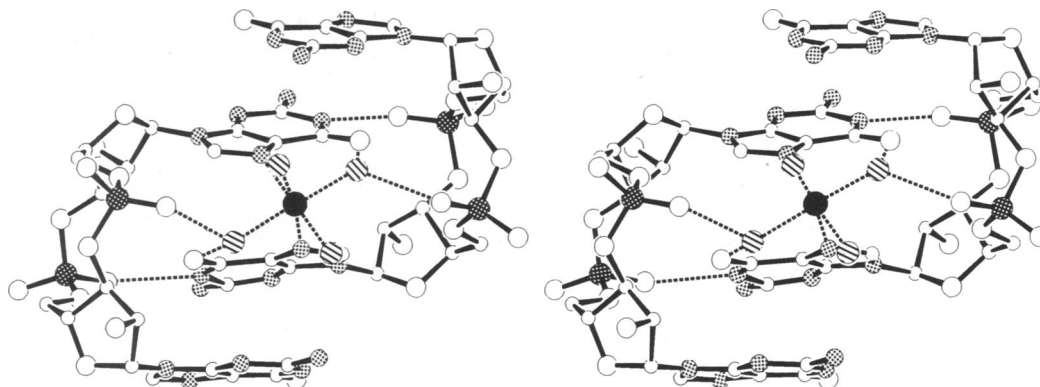


FIG. 4. An ORTEP stereoview emphasizing base-solvent and base-backbone hydrogen bonds of *c*-di-GMP. Nitrogen atoms and phosphorus atoms are stippled (black-on-white and white-on-black, respectively), the waters coordinated to the Mg^{2+} ion are hatched, the Mg^{2+} ion is black, and hydrogen bonds are included as dashed lines.

symmetry generates continuous interwoven stacks of intercalated units along the *c*-axis. The spacing between bases is 3.4 Å on average, equivalent to that seen in B-DNA.

The interaction between two intercalated molecules is stabilized not only by stacking of guanine bases but also by hydrogen bonds from the base of one molecule to the sugar phosphate backbone of the other. Almost linear hydrogen bonds (the N—O distances are 2.68 and 2.73 Å), which help to lock the two molecules together, are formed between the guanine endocyclic N1 atoms and the O2P oxygens of the adjacent phosphate groups. These interlocking hydrogen bonds are detailed in Fig. 4, which includes the hydrated Mg^{2+} complex. Two of the water molecules of the hydrated Mg^{2+} complex interact with both O2P atoms of phosphate groups that are not hydrogen-bonding to the base N1 atoms. They also form hydrogen bonds to the O6 atoms of the two central bases. The W—O2P (where W is water) distances are 2.64 and 2.73 Å and the W—O6 distances are 2.64 and 2.57 Å. Thus, this hydrated Mg^{2+} ion plays an integral role in the very tight interaction between molecules.

In addition to the interactions between the two cyclic molecules, there are G-G base-pairing interactions between molecules of adjacent stacks. These are shown with their detailed geometry in Fig. 5 and are described in Table 3. Central bases (residues 1 and 3) from two complexes form symmetrical purine-purine base pairs where N2 of one base is hydrogen-bonded to N3 of the other. The planes of these base pairs are buckled by about 35° (Fig. 5). The hydrogen-bond geometry of the two G-G base pairs is very similar due to the pseudo twofold symmetry of the intercalated complex. The other base pairs formed by the outer bases of the intercalated unit (residues 2 and 4) use an asymmetric purine-purine hydrogen-bonding scheme in which one purine donates two hydrogen atoms and the other receives them (Fig. 5). The two hydrogen bonds are formed between N1 and N7 and between N2 and O6, respectively. The angles C5—N7—N1 and C8—N7—N1 are 141° and 112° , respectively. This arrangement leads to a close contact between O6 of the guanine donating hydrogen atoms and C8 of the guanine receiving them. It should be noted that the hydrogen bond between N2 and O6 is slightly long (2.97 Å, Table 3). In contrast to the previous pairing, these base pairs are almost completely planar: the dihedral angles are 4° and the angles (C5—N7—N1—C6) are 168° . In addition, one of the outer guanines (residue 2) forms a buckled symmetric base pair with a guanine from a symmetry-related residue 2. The geometries of the two asymmetric G-G base pairs in crystallographically distinct environments are identical within standard deviations.

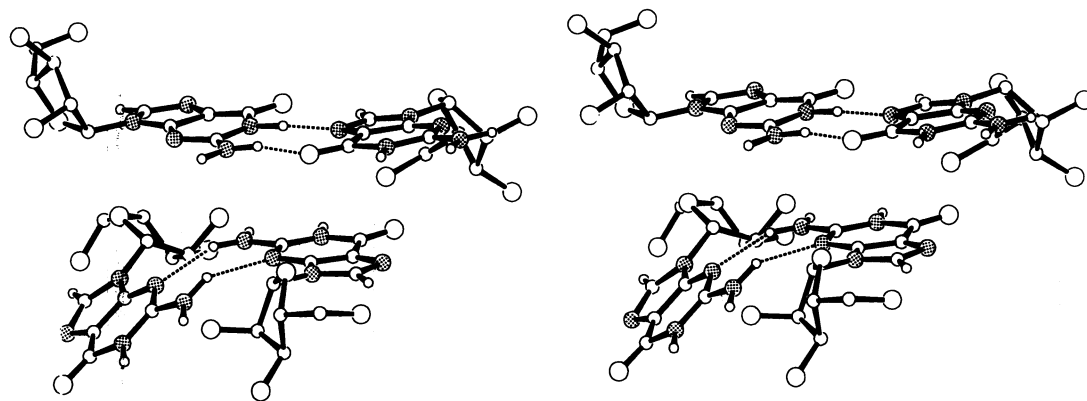


FIG. 5. An ORTEP stereoview of the intermolecular G-G base pairs in c-di-GMP. The four guanines shown are part of four different molecules. The diagram illustrates the vertical stacking between different molecules as well as the horizontal hydrogen bonding that stabilizes the stacks of cyclic dimers. The upper hydrogen-bonded pair shows the asymmetric hydrogen-bonding, with the guanine on the left donating two hydrogen atoms to the guanine on the right. A third potential C8—H···O6 hydrogen bond may exist between the two guanine residues. At the bottom the bent symmetrical G-G pairing is shown. Nitrogens are stippled and hydrogen bonds are drawn as dashed lines. Another guanine, which forms symmetric hydrogen bonds to N2 and N3 of the base at the upper left and is stacked on the guanine at the lower left, has been omitted for clarity.

DISCUSSION

The conformation of c-di-GMP demonstrates the flexible nature of the phosphodiester backbone of nucleic acids. The structural features of this cyclic ribonucleotide dimer are important for understanding nucleic acid conformations, such as loops and turns, which have been implicated in cellular regulation and nucleic acid processing (16). In addition, cyclic nucleic acids may represent common intermediates in a number of RNA-catalyzed reactions (17). This small RNA molecule exhibits those features necessary to cyclize such a molecule.

Previously we have determined the three-dimensional structure of a different cyclic dinucleotide, composed of DNA instead of RNA and adenines instead of guanines. In that structure the phosphodiester linkages assume a conformation very similar to the one observed here (18). However, the sugar pucker and glycosyl angles are different, resulting in two different orientations of the base planes. The 2' hydroxyl group of RNA introduces additional steric constraints in the sugar, resulting in less variability of RNA conformation compared to DNA. Therefore, one effect of the 2' hydroxyl group is less variability in the orientation of the bases relative to the backbone ring of cyclic dinucleotides. In a similar complex formed by the linear dinucleotide d(GpG), to which *cis*-diamminedichloroplatinum(II) has been covalently bound, the Pt²⁺ directly coordinates two guanine N7 atoms as the Mg²⁺ ion does in the present structure (19). In the platinum complex the metal ion produces a sharp kink in the dinucleotide backbone. In the current complex the bases are more nearly aligned and are still partially stacked. Thus, the tight binding of metals can influence stacking interactions and can introduce various degrees of helical distortions.

Telomeres generally contain stretches of G-rich sequences as has been determined biochemically for organisms ranging from tetrahymena to humans (4). At the 3' termini, there are single-stranded extensions of two or three copies of the characteristic G-rich sequence (20). This x-ray diffraction study provides an opportunity to analyze base-pairing modes between two guanines at atomic resolution. A number of models of the conformation and interactions of telomeric DNA have been proposed based on the electrophoretic mobility and the behavior of these sequences in solution (5, 6). In general the models involve G-G base pairs arranged in a square-planar tetrameric unit. Several x-ray fiber diffraction studies of guanine monomers and homopolymers have provided the basis for the hydrogen-bonding scheme used in these models (21–23). The fibers form four-stranded structures with asymmetric purine–purine base pairs, where O6 hydrogen-bonds to N1 and N7 to N2. However, only a limited number of examples of G-G base pairs have been observed in single-crystal x-ray diffraction studies of polynucleotides (24). In the present structure we can see two different examples of G-G base pairs, as shown in Fig. 5. The symmetric N2 to N3 pairing is the same as that observed in a number of B-DNA dodecamer crystal structures where the lattice is stabilized by hydrogen bonds from the two terminal base pairs of one helix to those of the next helix stacked above it (24).

One of the triple base pairs seen in yeast tRNA^{Phe} involves the 7-methylguanine at position 46 forming two hydrogen bonds to the guanine of the G²²·C¹³ base pair (31). That guanine–guanine base pairing is identical to the asymmetric base pairing shown at the top of Fig. 5.

The asymmetric base-pairing scheme is similar but not identical to that proposed for telomere interactions described

Table 3. Hydrogen-bond geometry of G-G base pairs in c-di-GMP

Base pair*	Donor	Acceptor	Distance, Å		Angle at H, degrees
			Donor–acceptor	H–acceptor	
G(1)·G(1') [†]	N2(1)	N3(1')	3.02	2.10	151
G(3)·G(3') [†]	N2(3)	N3(3')	3.00	2.09	149
G(2)·G(2') [†]	N2(2)	N3(2')	3.06	2.09	162
	N2(2')	O6(4)	2.95	1.99	158
G(4)·G(2')	N1(2')	N7(4)	2.84	1.84	172
	C8(4)	O6(2')	3.22	2.51	123

*The base numbers are given in parentheses: 1 and 3 are the inner bases, 2 and 4 are the outer bases of the intercalated dimer. Primed numbers designate symmetry-related molecules.

[†]These bases are related by crystallographic twofold rotation.

above. In our structure, the two hydrogen-bond donors are interchanged with respect to the acceptor atoms. Thus O6 is hydrogen-bonded to N2 and N7 to N1. The consequences of this switch in orientation are significant. N7 is the most basic nitrogen of guanine (pK_b 11.9), and a hydrogen bond to the relatively acidic nitrogen N1 (pK_a 9.2) is more stable than a hydrogen bond between N1 and O6. The bond between O6 and exocyclic N2 is similar to that seen in standard Watson-Crick base pairs between guanine O6 and cytosine N4. However, this orientation makes possible a third C—H \cdots O hydrogen bond between O6 of one guanine and the hydrogen atom at C8 of the other guanine. Such a bond would further strengthen the hydrogen bond between N1 and N7. The distance between the generated hydrogen at C8 (H8) and O6 is 2.52 Å. Although this is close to the sum of the van der Waals radii, it falls in the range that has been cited for a C—H \cdots O hydrogen bond (25–27). Thus there may be a weak C—H \cdots O hydrogen bond in this system. It is interesting that this hydrogen bond is not as significant in the crystal structures of guanine and guanosine, where the relative orientations of the bases are slightly different (28, 29). There, the distances between O6 and H8 are longer, 2.78 and 2.89 Å.

The observation of this hydrogen bond may be supported by NMR experiments. These show that in 2:1 mixtures of guanine and cytosine, there is a temperature dependence of the chemical shift of the hydrogen H8, implying its interaction in hydrogen bonding (30). This is not observed when the bases are mixed in 1:1 mixtures, suggesting that the three hydrogen bonds between guanines may be favored in G-rich sequences.

In the asymmetric hydrogen-bonding scheme, additional hydrogen bonds to guanine could be formed. This means that additional complexes could form with a larger number of members. This type of hydrogen-bonding network could stabilize those regions of cellular DNA where a number of guanine bases come together and form a stable complex.

We do not know whether the dimers of c-di-GMP, formed by self-intercalation and further stabilized by a hydrated Mg^{2+} , exist in solution, especially in the presence of a sufficient concentration of divalent cations. The spacing between two guanines in the same molecule is about 7 Å and it is thus a possible binding site for the side chains of aromatic amino acids. We can only speculate whether such an interaction with the membrane-bound cellulose synthase could induce a conformational change to initiate enzymatic activity.

We thank Dr. W. B. Schweizer from the Organic Chemistry Laboratory, Eidgenössische Technische Hochschule, Zurich, for help with the Cambridge Structural Database. M.E. acknowledges fellowship support from the Swiss National Foundation. This research was supported by grants from the National Institutes of Health, the American Cancer Society, the National Science Foundation, the Office of Naval Research, and the National Aeronautics and Space Administration.

1. Ross, P., Weinhouse, H., Aloni, Y., Michaeli, D., Weinberger-Ohana, P., Mayer, R., Braun, S., de Vroom, E., van der Marel,

- G. A., van Boom, J. H. & Benziman, M. (1987) *Nature (London)* **325**, 279–281.
2. Htun, H. & Dahlberg, J. E. (1988) *Science* **241**, 1791–1796.
3. Kohwi, Y. & Kohwi-Shigematsu, T. (1988) *Proc. Natl. Acad. Sci. USA* **85**, 3781–3785.
4. Blackburn, E. H. & Szostak, J. W. (1984) *Annu. Rev. Biochem.* **53**, 163–194.
5. Williamson, J. R., Raghuraman, M. K. & Cech, T. R. (1989) *Cell* **59**, 871–880.
6. Sundquist, W. I. & Klug, A. (1989) *Nature (London)* **342**, 825–829.
7. North, A. C. T., Phillips, D. & Matthews, F. S. (1968) *Acta Crystallogr. Sect. A* **24**, 351–359.
8. Sheldrick, G. M. (1986) in *Crystallographic Computing 3*, eds. Sheldrick, G. M., Krüger, C. & Goddard, T. (Oxford Univ. Press, Oxford), pp. 175–189.
9. Hendrickson, W. A. & Konnert, J. H. (1981) in *Biomolecular Structure, Conformation, Function, and Evolution*, ed. Srinivasan, R. (Pergamon, Oxford), pp. 43–57.
10. Jones, T. A. (1978) *J. Appl. Crystallogr.* **11**, 268–272.
11. Rabinovich, D. & Reich, K. (1979) SHELX76-400 (Weizmann Inst. of Science, Rehovot, Israel).
12. Maverick, E. (1985) BIGSHELX-76 (Univ. of California, Los Angeles).
13. Sheldrick, G. M. (1976) SHELX-76: *System of Computing Programs* (Univ. of Cambridge, Cambridge).
14. Johnson, C. K. (1976) ORTEP II (Oak Ridge National Lab., Oak Ridge, TN), Rep. ORNL-5138.
15. Kim, S. H., Berman, H. M., Seeman, N. C. & Newton, M. D. (1973) *Acta Crystallogr. Sect. B* **29**, 703–710.
16. Cech, T. R. & Bass, B. L. (1986) *Annu. Rev. Biochem.* **55**, 599–630.
17. Zaug, A. J., Kent, J. R. & Cech, T. R. (1984) *Science* **224**, 574–578.
18. Frederick, C. A., Coll, M., van der Marel, G. A., van Boom, J. H. & Wang, A. H.-J. (1988) *Biochemistry* **27**, 8350–8361.
19. Sherman, S., Gibson, D., Wang, A. H.-J. & Lippard, S. J. (1985) *Science* **230**, 412–417.
20. Henderson, E. R. & Blackburn, E. H. (1989) *Mol. Cell. Biol.* **9**, 345–348.
21. Gellert, M., Lipsett, M. N. & Davies, D. R. (1962) *Proc. Natl. Acad. Sci. USA* **48**, 2013–2018.
22. Sasisekharan, V., Zimmerman, S. & Davies, D. R. (1975) *J. Mol. Biol.* **92**, 171–179.
23. Zimmermann, S. B., Cohen, G. H. & Davies, D. R. (1975) *J. Mol. Biol.* **92**, 181–192.
24. Wing, R., Drew, H., Takano, T., Broka, C., Tanaka, S., Itakura, K. & Dickerson, R. E. (1980) *Nature (London)* **287**, 755–758.
25. Taylor, R. & Kennard, O. (1982) *J. Am. Chem. Soc.* **104**, 5063–5070.
26. Jeffrey, G. A., Maluszynska, H. & Mitra, J. (1985) *Int. J. Biol. Macromol.* **7**, 336–348.
27. Seiler, P. & Dunitz, J. D. (1989) *Helv. Chim. Acta* **72**, 1125–1135.
28. Bugg, C. E., Thewalt, U. T. & Marsh, R. E. (1968) *Biochem. Biophys. Res. Commun.* **33**, 436–440.
29. Thewalt, U. T., Bugg, C. E. & Marsh, R. E. (1970) *Acta Crystallogr. Sect. B* **26**, 1089–1101.
30. Williams, N. G., Williams, L. D. & Shaw, B. R. (1989) *J. Am. Chem. Soc.* **111**, 7205–7209.
31. Rich, A. & RajBhandary, U. L. (1976) *Annu. Rev. Biochem.* **45**, 805–860.